



Los Angeles, London, New Delhi
and Singapore
<http://www.sagepub.com>



© The Author(s), 2010. Reprints and permissions:
<http://www.sagepub.co.uk/journalsPermissions.nav>

ISSN 0734-242X

Waste Management & Research

2010: 28: 364-372

DOI: 10.1177/0734242X09357079

The application of magnetic gradiometry and electromagnetic induction at a former radioactive waste disposal site

Dale Franklin Rucker

Arcadis US, Inc., Tucson, Arizona, USA

A former radioactive waste disposal site is surveyed with two non-intrusive geophysical techniques, including magnetic gradiometry and electromagnetic induction. Data were gathered over the site by towing the geophysical equipment mounted to a non-electrically conductive and non-magnetic fibre-glass cart. Magnetic gradiometry, which detects the location of ferromagnetic material, including iron and steel, was used to map the existence of a previously unknown buried pipeline formerly used in the delivery of liquid waste to a number of surface disposal trenches and concrete vaults. The existence of a possible pipeline is reinforced by historical engineering drawing and photographs. The electromagnetic induction (EMI) technique was used to map areas of high and low electrical conductivity, which coincide with the magnetic gradiometry data. The EMI also provided information on areas of high electrical conductivity unrelated to a pipeline network. Both data sets demonstrate the usefulness of surface geophysical surveillance techniques to minimize the risk of exposure in the event of future remediation efforts.

Keywords: magnetic gradiometry, electromagnetic induction, surveillance, geophysics, radioactive waste disposal

Introduction

Radioactive waste disposal strategies have changed significantly over the past half-century, and appear to evolve continuously to minimize risk to future populations. These strategies have included direct disposal to the biosphere (Gephart 2003), interim storage (Hylko *et al.* 1989), reprocessing (Cometto *et al.* 2004), and long-term (near surface, deep, and very deep) geological disposal of a high-integrity waste form (Lennemann *et al.*, 1976, Gibb 1999). Direct disposal, including the radiological release of liquid waste to unlined trenches and bottomless concrete vaults, is the least effective disposal strategy. With specific retention (Joussein *et al.* 2004), the waste was thought to bind with the soil and be prevented from migrating sufficiently from the disposal area. It has been shown, however, that waste can leach from the most sorptive material (Rameback *et al.* 2000). To date, it is the prevailing belief among top nuclear agencies that deep geological disposal is the safest form of disposal (IAEA 1994, OECD/NEA 1995).

The question arises, then, of what to do with the legacy waste disposal sites that do not conform to the current understanding of safe disposal. Many of these sites are

equipped with continuous monitoring programmes to track the migration of radionuclides and other hazardous constituents from the original source location (Poston *et al.* 2000). This option, however, could prove to be costly due to the indefinite nature of long-term monitoring. Another option includes re-disposal, where waste and waste containers are removed from their present location and disposed in repositories that provide a safe containment for 10,000 years or more. One such site is the TRU Waste Burial Grounds on the Hanford Site (State of Washington, USA) (McDonald 1999), where waste drums are being removed from interim storage and re-disposed at the Waste Isolation Pilot Plant.

Prior to removing radioactive waste and waste containers, a proper site evaluation and characterization should be performed. The site evaluation process would simply be to review institutional knowledge regarding the specific disposal site, such as issued reports and published papers. Site characterization, on the other hand, would require gathering additional information to discern differences between expected and actual disposal conditions. Site characterization is especially

Corresponding author: Dale Franklin Rucker, Arcadis US, Inc., Tucson, AZ 85716, USA.

E-mail: druck8240@gmail.com

Received 18 September 2009; accepted in revised form 13 November 2009

Figures 1, 3 appear in color online: <http://wmr.sagepub.com>

important when institutional knowledge of legacy disposal sites has been lost. Gephart (2003) reported that conflicting information exists regarding the number and placement of radiological waste disposal sites at the Hanford Site. To increase knowledge and reduce uncertainty regarding the size and location of the legacy disposal sites, a non-intrusive geophysical survey is recommended.

Environmental geophysics is the measurement of physical properties of the shallow earth to characterize and remediate environmental problems (Sheriff 2002). These properties could be electrical (conductivity, dielectric), magnetic (susceptibility, permeability), or a host of others. For a comprehensive review of geophysical methods, the reader is referred to Telford *et al.* (1995). Geophysics has been applied extensively to buried hazardous waste sites (see Ward 1990, Gullien & Hertzog 2004) to distinguish landfill boundaries and differentiate the various types of waste. The most effective geophysical methods have been magnetic gradiometry and electromagnetic induction. Coupled, these two methods can locate the existence of ferromagnetic steel and iron, non-ferrous metals, and conductive fluids that may have leached from the landfill. Siegrist *et al.* (1989) presented a combined (*i.e.* acquired separately) electromagnetic and magnetic survey over an industrial site to locate drums. Their work was limited in scope and coverage area. Doll *et al.* (2000) presented a simultaneous magnetic gradiometry and electromagnetic induction survey from a helicopter over the Oak Ridge Facility. Their work demonstrated that areas containing disposed waste drums could be found effectively over a nuclear facility.

Although useful as a regional reconnaissance tool, the method of Doll *et al.* (2000) could not distinguish individual trenches where metal was known to exist. The low resolution of the instrumentation was a limiting factor, as was transient environmental noise from sources such as vehicles parked within the flight line and above-ground power lines. A geophysical survey conducted directly on the surface would be minimally affected by these issues, as demonstrated by Siegrist *et al.* (1989). This study presents electromagnetic and magnetic geophysical data collected on the surface over a known disposal waste site and differs from previous studies in combined resolution and scale. The site was thought to be free of metal debris, but was determined otherwise after analyses of the data. The objective of this study was to demonstrate the methodology of collecting and interpreting high resolution data obtained in a radiologically controlled area. The method is useful for personnel interested in locating the position of debris metal waste without the risk and expense of ground probing or drilling. For example, Rucker *et al.* (2010) showed that excessive infrastructure can inhibit the use of surface-based resistivity and the knowledge of location and density of buried metallic debris may avoid unnecessary costs.

Background

Magnetic gradiometry

Magnetometry is the study of the earth's magnetic field and is the oldest branch of geophysics (Telford *et al.* 1995). The

earth's field is composed of three parts: (i) the main field, which is internal, *i.e.* from a source from within the earth that varies slowly in time and space; (ii) a secondary field that is external to the earth and varies rapidly in time; and (iii) small internal fields constant in time and space that are caused by local magnetic anomalies in the near-surface crust. Of interest to the environmental geophysicists are these localized anomalies. The anomalies are caused either by magnetic minerals (mainly magnetite or pyrrhotite) or buried steel and are the result of contrasts in the magnetic susceptibility (k). The average values for k are typically less than 1 for sedimentary formations and upwards to 20,000 for magnetite minerals.

The magnetic field is measured with a magnetometer. Magnetometers permit rapid, non-contact surveys to locate buried metallic objects and features. Portable (one-person) field units can be used virtually anywhere that a person can walk, although, they may be sensitive to local interferences, such as fences and overhead wires. Airborne magnetometers are towed by aircraft and are used to measure regional anomalies. Field-portable magnetometers may be single- or dual-sensor. Single-sensor magnetometers measure total field. Dual-sensor magnetometers, depending on their configuration, can be used to measure the total field at multiple vertical or horizontal offsets along the measurement path, or as a gradiometer. A gradiometer typically uses two sensors to measure the gradient in the magnetic field. The magnetic gradient allows the differentiation between deeply buried objects versus those that are superficially buried.

Magnetic surveys are typically run with two separate magnetometers. The first magnetometer is used as a base station to record the earth's primary field and the diurnally changing secondary field. The second magnetometer is used as a rover to measure the spatial variation of the earth's field and may include various components (*i.e.* inclination, declination, and total intensity). By removing the temporal variation and the static value of the base station from that of the rover, one is left with a residual magnetic field that is the result of local spatial variations only.

The shortcoming with most magnetometers is that they only record the total scalar magnetic field, F , and not the separate components of the vector field. This shortcoming can make the interpretation of magnetic anomalies difficult, especially since the strength of the field between the magnetometer and target is reduced as a function of the inverse of distance cubed. Additional complications can include the inclination and declination of the earth's field, the presence of any remnant magnetization associated with the target, and the shape of the target.

Electromagnetic induction

Earth materials have the capacity to transmit electrical currents over a wide range, and depend on the material properties of electrical conductivity and magnetic permeability (or susceptibility). Electrical conductivity is a function of soil type, porosity, saturation, dissolved salts, and frequency of

the induced signal (Telford *et al.* 1995); magnetic permeability is dependent upon the presence of magnetic materials. For example, clay will transmit electrical current more readily (*i.e.* higher conductivity) than sand; saturated soils have higher conductivity than desiccated soils. Electromagnetic methods seek to identify various earth materials by measuring their electrical characteristics and interpreting results in terms of those characteristics.

Electromagnetic induction methods employ a transmitting coil and a receiving coil. The transmitting coil induces eddy currents in the earth through a primary magnetic field, which themselves generate secondary magnetic fields that are affected by the earth materials within the excited zone. Some parts of the secondary fields are intercepted by the receiving coil, resulting in an output voltage proportional to the terrain conductivity within the zone. By moving these coils laterally, variations in conductivity or permeability can be interpreted to find various buried features. The transmitting coil frequency and the distance between transmitting coil and receiving coil determine the depth of investigation; the output permits construction of a stratigraphic profile of intervening depth.

The received signal comprises an in-phase (real) and quadrature (imaginary) component, relating, respectively, to the magnetic permeability and electrical conductivity of the ground (Huang & Won 2004). These data are usually presented as the ratio of the secondary field (received) to the primary field (transmitted) multiplied by 10⁶ (Ward & Hohmann 1988). The units of the relative measure are in parts per million. Instrumentation for the electromagnetic induction method can include co-axial or co-planar transmitting-receiving coils. The coils for a co-axial system can be housed within a rigid ski at a fixed distance and operate at multiple frequencies simultaneously (Huang & Won 2000).

Methodology

A geophysical reconnaissance survey, including magnetic gradiometry (MAG) and electromagnetic induction (EMI), was conducted at the BC Cribs and Trenches Area within the US Department of Energy Hanford Site in south-eastern Washington (Figure 1). The area is a legacy disposal site used during the mid-1950s to dispose liquid wastes generated during the uranium recovery and ferrocyanide processes at the

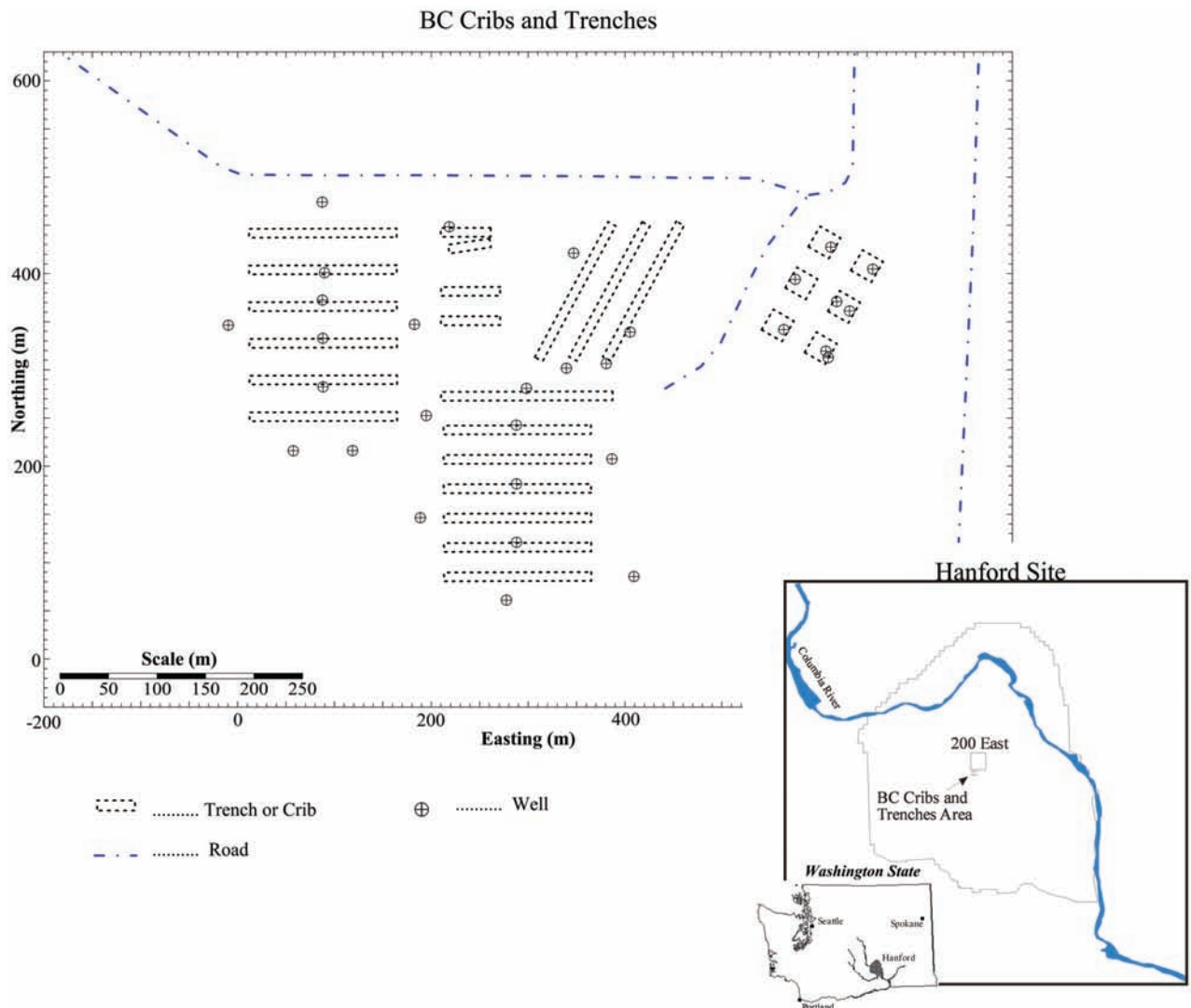


Fig. 1: BC cribs and trenches area at the Hanford site, Richland, WA, USA.

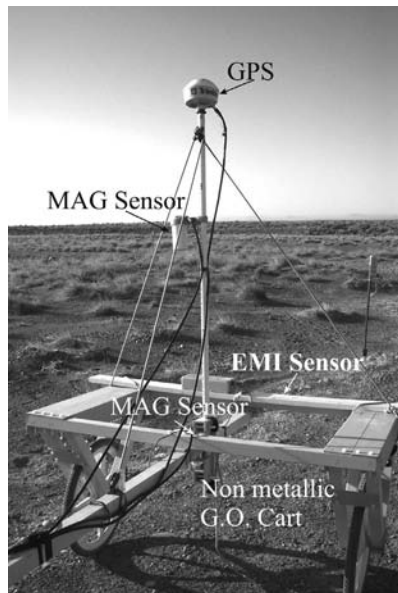


Fig. 2. Photograph of G.O. Cart used to tow the magnetic gradiometry sensors, electromagnetic induction sensor, and GPS.

200-TW-1 operable unit (DOE-RL, 1988). During this period, the most thermally loaded wastes were disposed in 16 open, unlined trenches and six bottomless concrete vaults (cribs), which are scattered over an area of 20 ha. Approximately 115,000 m³ of liquid effluent was delivered to the disposal area by a large steel pipeline and included the largest inventory of technetium-99 ever disposed to the soil at the Hanford Site (Ward *et al.* 2004). Rucker & Fink (2007) and Rucker *et al.* (2009) have presented the results of the plume resulting from the legacy disposal.

To acquire data for the MAG and EMI survey, an all-terrain vehicle (ATV) was used to tow a Geophysical Operations Cart (G.O. Cart), constructed of fibre-glass, nylon, and plastic so as to not interfere with the geophysical equipment (Figure 2). The MAG and EMI data were acquired along parallel lines spaced approximately 2–3 m apart. The speed of the ATV was controlled such that a nominal sampling rate of three measurements per metre was attained. A 5-m extended tongue was used to distance the ATV from the G.O. Cart. Geographic control for the MAG and EMI data was established using a Trimble AgGPS 132 navigation system. The differential GPS receiver was mounted approximately 1.5 m above the G.O. Cart on a fibre-glass rod. The GPS was connected directly to the MAG console for data-logging capabilities and the sampling rate of the GPS was fixed at one reading per second. The accuracy of the differential GPS is within 1 m.

Magnetic gradiometry

For the MAG investigation, a Geometrics G-858 caesium vapour gradiometer was used to collect the total magnetic field and magnetic gradient data across the site, and was used for the rover magnetometer. As a gradiometer (dual sensor),

the sensors for the G-858 were spaced vertically 1 m apart with the lowest sensor being approximately 1 m from the ground surface. In addition, the sensors were oriented vertically. A data-logger and a control console, which was mounted in front of the driver, were used to control the data collection on the ATV. Data were recorded to an accuracy of 0.2 nano-Teslas (nT) in the range 20,000–120,000 nT at discrete time intervals of five readings per second. Time, date, and magnetic readings (magnetic field for the top sensor, magnetic field for the bottom sensor, and magnetic gradient) were stored in a data-logger and down-loaded to a laptop PC for processing. A Geometrics G-856 proton precession magnetometer was used for the base station. The base magnetometer consisted of a kerosene-filled sensor, which was connected to a data-logger and 12-V battery. Data were typically recorded at a sampling rate of 5 s.

Post processing of the MAG data included the removal of the base station effects from the rover (referred to as diurnal correction), geo-referencing, correcting for heading errors, and filtering. For geo-referencing, the GPS data were linearly interpolated to the position of the MAG data using the time stamp for each measurement as the independent variable. The diurnal correction included low-pass filtering of the base station data to remove spikes. The diurnal data (with mean 54,748 nT) was then subtracted from the rover MAG data to calculate the magnetic field due to anomalies.

Heading error in the MAG data results in the preferential alignment of the sensors in the earth's magnetic field. Heading errors are the cause of anomalous readings unrelated to any response from buried metallic debris. The error associated with heading was calculated from the MAG data collected in eight distinct directions; data were collected every 45° from a northerly heading. A curve was fit for the direction of travel versus field strength for each sensor (Figure 3), which was subsequently subtracted from the data.

After correcting the MAG data for heading errors, the data were passed through a low-pass 2-D spatial filter to remove high-frequency noise. Additionally, coincident data points (within 0.03 m) were removed to eliminate redundancy. Coincident data points were collected when the G.O. Cart was stationary while the instruments continued to collect data.

Electromagnetic induction

Multifrequency electromagnetic data were collected using a Geophex GEM-2 electromagnetic conductivity and susceptibility instrument (Huang & Won 2000). The GEM-2 consists of a sensor housing (ski) and electronics console. The ski was positioned broadside on the back of the G.O. Cart (*i.e.* the transmitter and receiving coils were orthogonal to direction of travel). The coils were separated 1.66 m apart and were horizontally placed on the G.O. Cart (*i.e.* vertical axis coils). The electronics console was connected directly to the G-858 console for data-logging capabilities. Both in-phase and quadrature data were collected at five frequencies ranging from 5–20 kHz.

The first step in processing the EMI data is geo-referencing of each data point with the differential GPS. The GPS

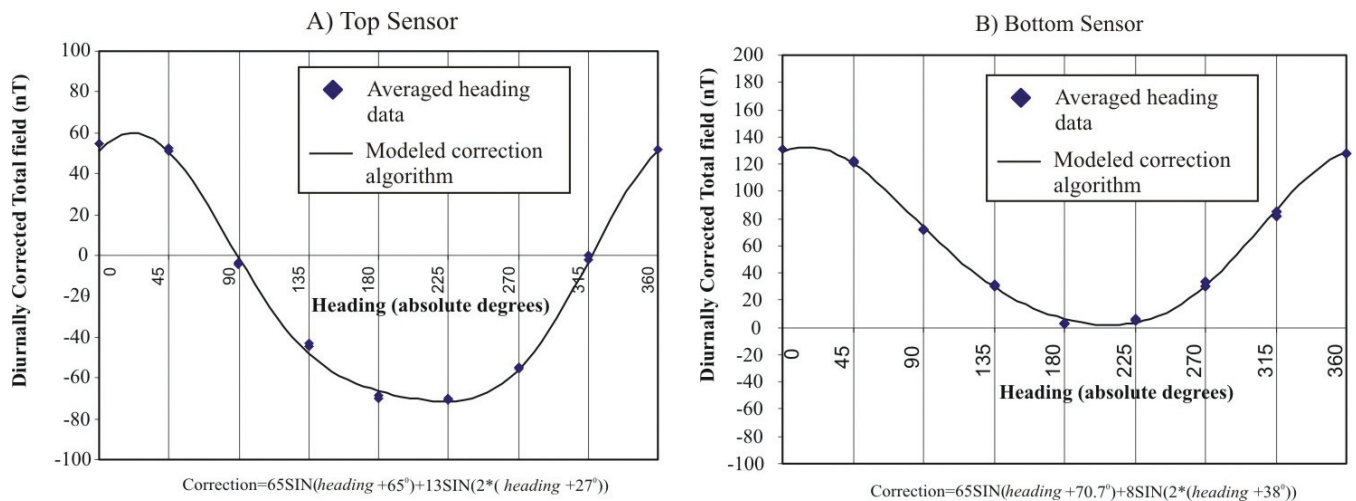


Fig. 3: Heading error correction for MAG data. (A) Upper sensor. (B) Lower sensor.

data were recorded at a sampling rate of one measurement per second, whereas the GEM-2 EMI data were recorded at a rate of three measurements per second. Linear interpolation was used to geo-reference every EMI data point using the time stamp from both instruments as the independent variable.

After geo-referencing, the in-phase and quadrature data were run through an inversion algorithm (Huang & Won 2000). The inversion algorithm converted the measured data to magnetic susceptibility and electrical conductivity. The results were susceptibility data for each of the five frequencies, electrical conductivity for each of the five frequencies, and a total electrical conductivity (average conductivity from all five frequencies). After geo-referencing, the data were shifted for the day-to-day bias in the data. The bias was calculated from a coincident data collection run at the beginning of each collection day. Slight differences in the daily data records can be attributed to environmental or instrument set-up changes.

After correcting the GEM-2 EMI data for each of the time-series issues, the data were compiled spatially and passed through a low-pass 2-D spatial filter to remove high-frequency noise. Additionally, coincident data points (within 0.03 m) were removed to eliminate redundancy. Coincident data points were collected when the G.O. Cart was stationary while the instruments continued to collect data.

Results

Magnetic gradiometry

Figure 4 is a contour map of the vertical magnetic gradient, which was calculated by subtracting the total magnetic field of the upper sensor at 2 m above the ground surface from the total magnetic field acquired with the lower sensor located 1 m above the ground surface. The contour map was compiled from 375,726 data points that were kriged on a 1-m square grid. The kriging semi-variogram was linear. Figure 4 shows several pronounced circular and linear magnetic gradient anomalies. The circular features show an extreme negative

response in the magnetic gradient field, in particular around the monitoring wells. The negative response is a result of ferrous metallic objects (steel well casing) being located above ground, *i.e.* the perturbation in the magnetic field was larger in the upper sensor than the lower sensor. The relative size of the circular anomalies was the direct result of how close the G.O. Cart came to the metallic obstruction. Measurements closer to the well casing show a much larger magnetic response than those that were farther away.

The linear features in Figure 4 are possibly a result of a distributed network of pipes. In particular, the pipelines within the cribs (north-east portion of the site) are very well defined. Figure 5 shows a close-up of the magnetic gradient in the cribs area (Figure 5A) and an interpretation of the anomalous features taken from engineering drawings (Figure 5B). From the drawings, it was shown that a steel pipe delivered liquid effluent from the north. The pipeline network then distributed waste to the cribs and the trenches to the west of the cribs by way of an iron gate valve. From this valve, steel pipe was used to move waste to a siphon tank. The tank, made of steel, shows an extremely large response in the MAG contour map. Continuing from the siphon tank, waste was moved to each of the six cribs through a distribution manifold system with more valves controlling the waste received by a specific crib. Each crib contained a waste distribution structure of wood timbers and a steel plate that was surrounded by gravel placed in an excavation approximately 3 m deep. The engineering drawings indicated that the excavation was approximately 4 m deep with sloping sides and a bottom area of approximately 150 m². The contours of the magnetic gradient show these steel forms distinctly from those anomalies related to the monitoring wells.

Other similar linear features can be seen throughout the site within the trenches. A map interpreting the location of these pipelines is presented as Figure 6. Specifically, trenches 216-B-33 and 216-B-34 in the western portion of the site show linear features connecting on the east side to a common pipeline

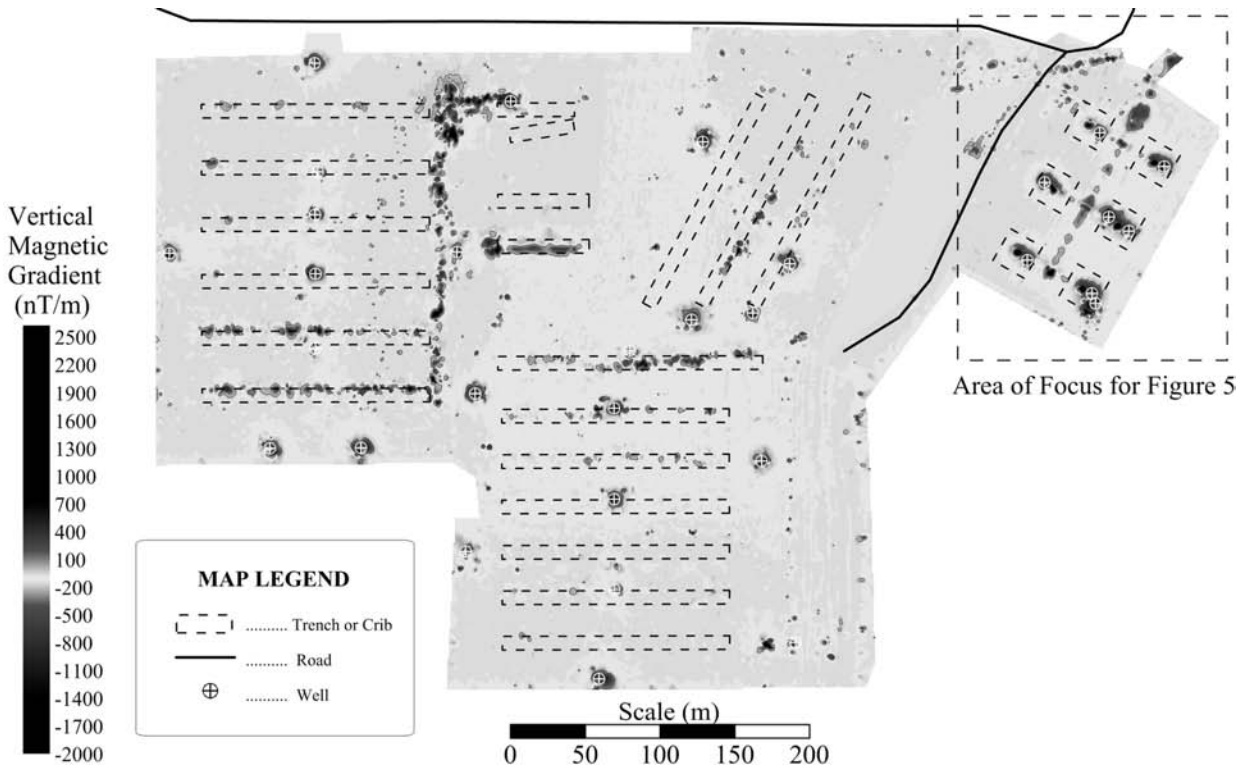


Fig. 4: Magnetic gradient (nT m^{-1}) at the BC cribs and trenches area.

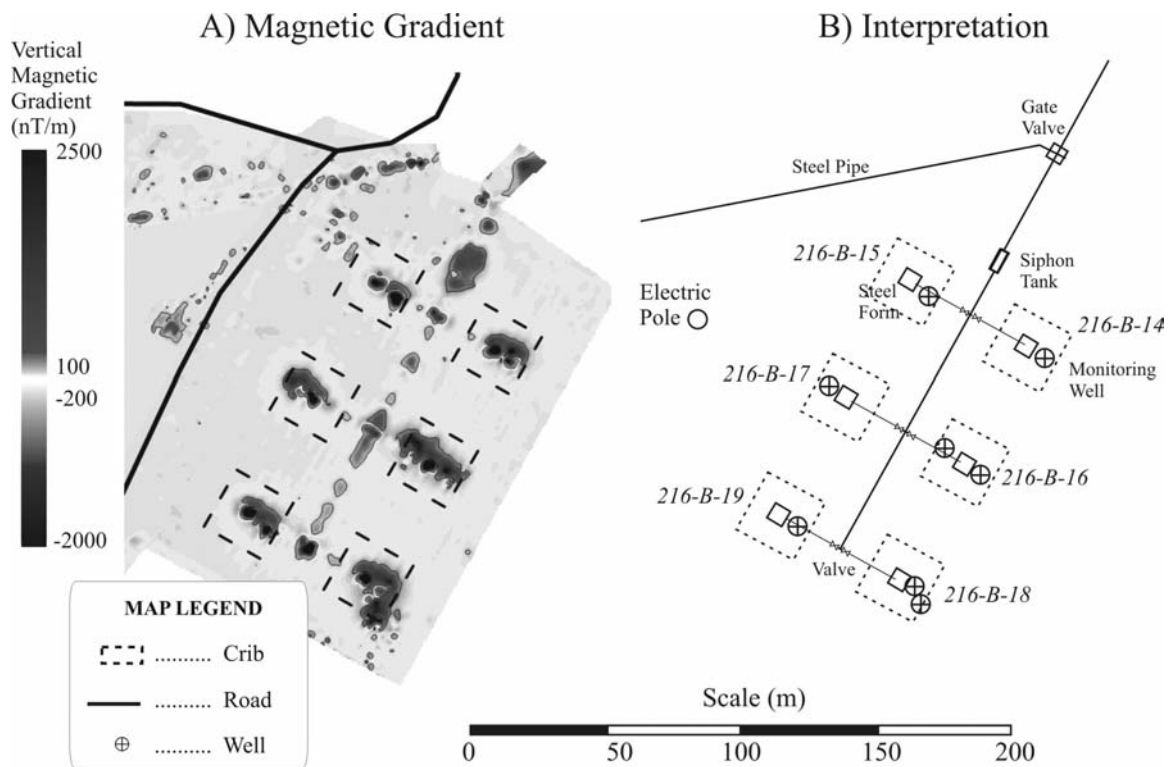


Fig. 5: (A) Magnetic gradient (nT m^{-1}) over the cribs area. (B) Interpretation of anomalies from engineering drawings of the site.

that runs north towards 216-B-29. A large anomaly also exists to the east of trench 216-B-29. Due to the large disturbance in the magnetic field at this location, it is possible that (i) several buried pipes, (ii) valves, or (iii) one large pipe could exist just

below the surface. It is known that trenches 216-B-53A, B, 216-B-54, and 216-B-58 were used approximately 10 years later than the other trenches and cribs around the site. Therefore, it is unlikely that the pipeline that distributed waste to

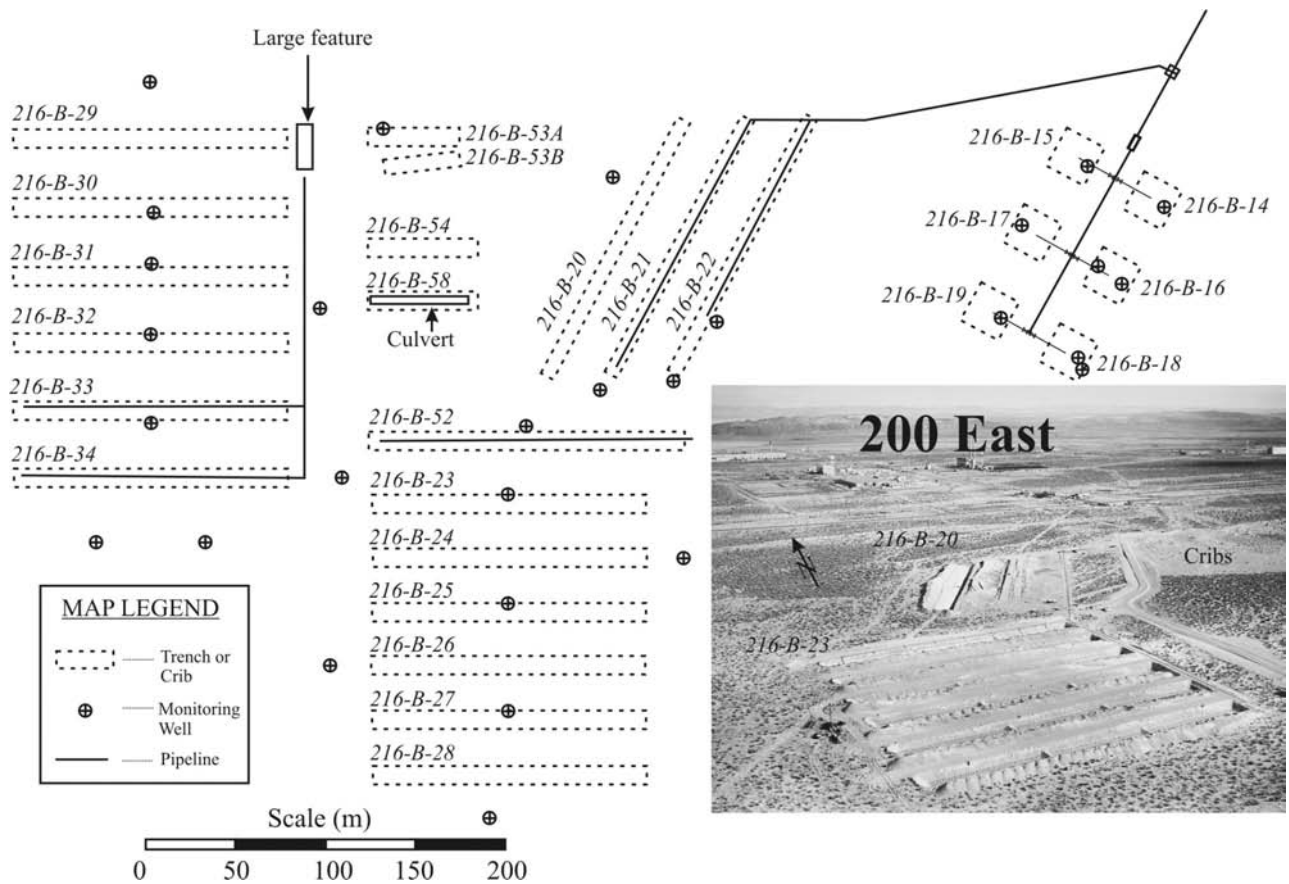


Fig. 6: Locations of buried pipes and historical photograph (1956) at the BC cribs and trenches area.

trenches 216-B-33 and 216-B-34 are connected to 216-B-53A. The large feature beneath 216-B-58 is a buried culvert discovered in other engineering drawings.

The existence of other abandoned pipelines can be seen in the centre of the site within trenches 216-B-21, 216-B-22, and 216-B-52. A historical photograph taken during the construction of the site (1956) shows many these trenches just after excavation (Figure 6). The photograph shows that the pipeline was placed in all the trenches at once. The MAG data do not confirm this observation, suggesting that the pipeline was removed from several of the trenches after disposal. One possible explanation is that the pipes were re-used in the trenches in the western portion of the site (216-B-29 through 216-B-34) and abandoned there.

Electromagnetic induction

The electrical conductivity, as calculated from the quadrature data collected with the EMI sensor, is presented in Figure 7. The data are contoured from a kriged data set with similar parameters as the MAG data of Figure 4 (linear semi-variogram and 1-m regular grid). A total of 166,067 data points were used to compile Figure 7. The reduced number of data points is the result of the sampling rate of the EMI sensor (three samples per second) relative to that of the MAG sensor (five samples per second).

Figure 7 shows several pronounced features that have a higher electrical conductivity relative to the background. In

particular, the cribs area in the north-east portion of the site shows a strong anomaly where the steel pipeline was identified from the engineering drawings shown in Figure 5. Additionally, the siphon tank and the pipeline that ran from the gate valve to the diagonal trenches in the centre of the site appears within the EMI data. Other linear features that coincide with interpreted pipelines from Figure 6 include that of trenches 216-B-33, 216-B-34, 216-B-52, and the larger feature to the east of 216-B-29.

In addition to the anomalies that are tied directly to specific trenches or cribs, there are a couple of zones showing high electrical conductivity. These include areas between trenches 216-B-29 and 216-B-30 and at the end of the road that is immediately west of the cribs area. Both zones could be the result of increased ionic strength due to the addition of solvents or a highly concentrated salt solution. However, there has been no verification of these observations. On the other hand, it is highly unlikely that the increased conductivity is the result of buried metal since neither area appeared in the MAG data.

Alternatively, there are areas scattered around the site with extremely low electrical conductivity which could be the result of an absence of moisture or salts. These areas can be seen to the east side of the trenches in the southern portion of the site (216-B-26) and directly north of the cribs. Rucker & Sweeney (2004) have shown that direct-current electrical resistivity measurements in these regions consist of low elec-

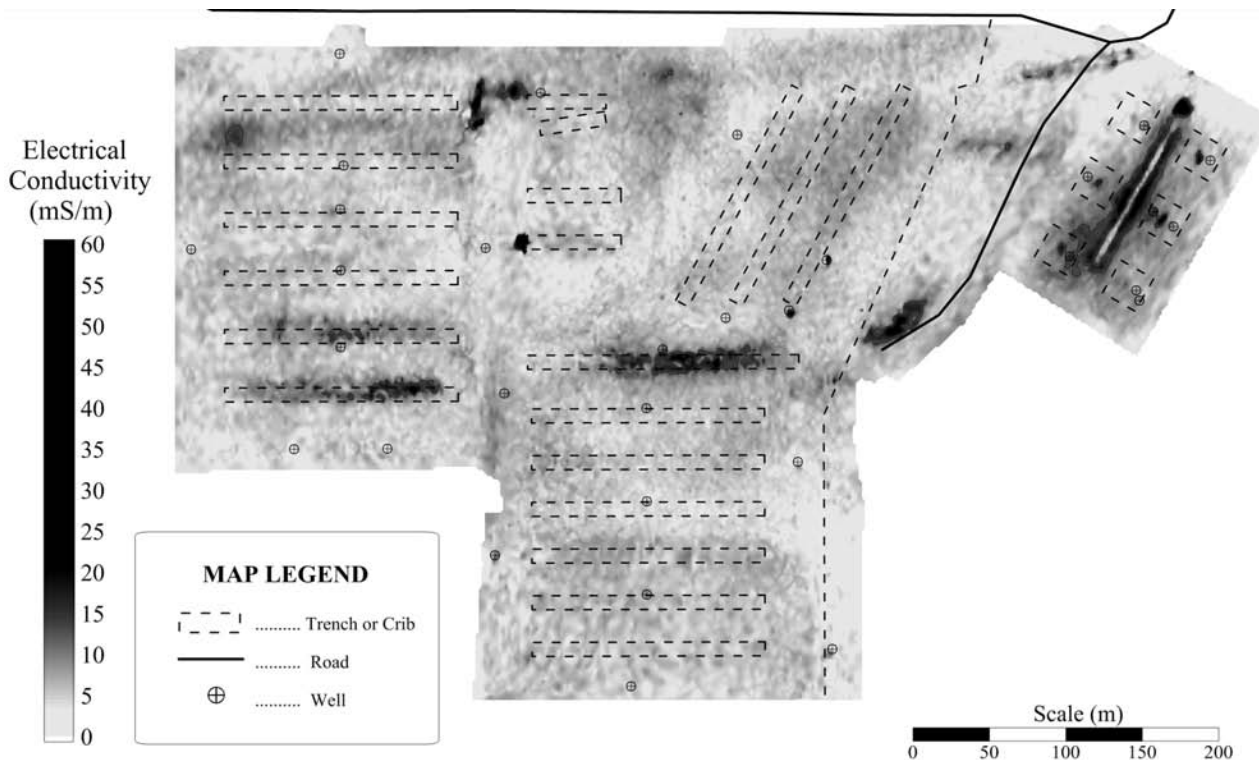


Fig. 7: Electrical conductivity at 10 kHz (mS m^{-1}) at the BC cribs and trenches area.

trically conductive material that is more common to the natural formation. Additional data are being collected to test whether the moderate-to-high electrical conductivity values (greater than 5 mS m^{-1}) can be linked directly to previous disposal activities.

Conclusions

A geophysical reconnaissance survey was conducted over a legacy waste site to identify subsurface anomalous features related to past disposal activities, including steel, iron, or solvents. Liquid high-level radioactive liquid waste was delivered to the site by way of a steel pipeline from a reactor located to the north of the site. A series of unlined trenches and cribs received the waste under the semblance of specific retention in the hopes that the radiological constituents would absorb to the soil matrix. Sorption would prevent the underlying groundwater from being contaminated with the waste.

The geophysical surveys included magnetic gradiometry and electromagnetic induction. The methods were deployed simultaneously by mounting the sensors to a non-electrically conductive and non-magnetic cart, which was towed by an ATV. The data were geo-referenced with a differential GPS, also mounted on the cart. The use of the cart allowed spatial high-resolution data to be collected in a relatively short period of time ($> 450,000$ data points within 20 ha and collected within 10 days).

The magnetic gradiometry, calculated by subtracting the total magnetic field of the upper sensor from the total magnetic field of the lower sensor, showed several circular and linear features. The features manifested themselves as extreme

positive ($> 2000 \text{ nT m}^{-1}$) or extreme negative ($< -1000 \text{ nT m}^{-1}$) values indicative of dipolar responses frequently observed with magnetic anomalies. Magnetic anomalies are the result of material contrasts in magnetic susceptibility. The circular features are coincident with steel-cased wells that stick above ground approximately 1 m. The relative size of the anomaly was the direct result of how close the cart came to the metallic obstruction.

Linear magnetic anomalies in the cribs area (north-east portion of the site) were most likely the result of a steel pipeline, siphon tank, and iron valves used to deliver and control waste flow to the individual cribs. These features were coincident with engineering drawings of the site, which explicitly showed the various components in the area. Similar linear magnetic features were identified in other areas of the site and were thought to originate from underground pipelines that delivered waste to the trenches. Although no engineering drawings were available for direct comparison, a historical photograph shows open trenches that could have received waste from a pipe.

The electrical conductivity, collected with the electromagnetic sensor at 10 kHz, repeated many of the findings of the magnetic gradiometer, including linear features associated with interpreted pipelines. However, when compared to the magnetic gradiometer, the EMI data appeared to be of lower spatial resolution. The EMI response from the pipelines, for example, appear to be larger than the width of the trench, so the exact location of the pipeline is uncertain. Huang & Won (2000), on the other hand, suggest that the resulting data of a multi-frequency EMI is better than that of a magnetometer

alone, providing a greater resolution. Unlike the magnetic gradiometer, the electrical conductivity data can provide insight into non-metallic features such as the addition (or absence) of a high ionic strength solution that was disposed at the site. Together, the tools provide a rapid reconnaissance of waste sites that can minimize impact to further investigations (e.g. drilling or electrical resistivity) or remediation.

References

- Cometto, M., Wydler, P. & Chawla, R. (2004) A comparative physics study of alternative longterm strategies for closure of the nuclear fuel cycle. *Annals of Nuclear Energy*, **31**, 413–429.
- Doll, W.E., Nyquist, J.E., Beard, L.P. & Gamey, T.J. (2000) Airborne geophysical surveying for hazardous waste site characterization on the Oak Ridge Reservation, Tennessee. *Geophysics*, **65**, 1372–1387.
- Gephart, R.E. (2003) *Hanford, A conversation about nuclear waste and cleanup*. Battelle Press, Richland WA.
- Gibb, F.G.F. (1999) High-temperature, very deep, geological disposal: a safer alternative for high-level radioactive waste? *Waste Management*, **19**, 207–221.
- Guillen, D.P. & Hertzog, R.C. (2004) A survey of Department of Energy-sponsored geophysical research for shallow waste site characterization. *Vadose Zone Journal*, **3**, 122–133.
- Huang, H. & Won, I.J. (2000) Conductivity and susceptibility mapping using broadband electromagnetic sensors. *Journal of Environmental and Engineering Geophysics*, **5**, 31–41.
- Huang, H. & Won, I.J. (2004) Electromagnetic detection of buried metallic objects using quad–quad conductivity. *Geophysics*, **69**, 1387–1393.
- Hylko, J.M., Brennan, W.P. & Setlur, A.V. (1989) Status of interim spent fuel storage technologies at commercial nuclear power plants. *Nuclear Plant Journal*, **7**, 1–4.
- International Atomic Energy Agency (IAEA). (1994) *Siting of geological disposal facilities*, Safety Series No. 111-G-4.1. Vienna, Austria.
- Joussein, E., Kruyts, N., Righi, D., Petit, S. & Delvaux, B. (2004) Specific retention of radiocesium in volcanic ash soils devoid of micaceous clay minerals. *Soil Science Society of America Journal*, **68**, 313–319.
- Lennemann, W.L., Parker, H.E. & West, P.J. (1976) Management of radioactive wastes. *Annals of Nuclear Energy*, **3**, 285–295.
- McDonald, K.M. (1999) *Transuranic (TRU) Waste Phase I Retrieval Plan*. HNF-4781. Fluor Daniel Hanford, Inc. Report to the US Department of Energy, Richland, WA.
- Organization for Economic Co-operation and Development/Nuclear Energy Agency (OECD/NEA). (1995) *The environmental and ethical basis of geologic disposal. A collective opinion of the NEA Radioactive Waste Management Committee*. Paris, France.
- Poston, T.M., Hanf, R.W. & Dirkes, R.L. (eds) (2000) *Hanford Site Environmental Report for Calendar Year 1999*. PNNL-13230, Pacific Northwest National Laboratory, Richland, WA.
- Rameback, H., Albinsson, Y., Skalberg, M., Eklund, U.B., Kjellberg, L. & Werme, L. (2000) Transport and leaching of technetium and uranium from spent UO₂ fuel in compacted bentonite clay. *Journal of Nuclear Materials*, **277**, 288–294.
- Rucker, D.F. & Sweeney, M.D. (2004) *Plume Delineation in the BC Cribs and Trenches Area*. Pacific Northwest National Laboratory, PNNL-14948. Richland, WA.
- Rucker, D.F. & Fink, J.B. (2007) Inorganic plume delineation using surface high resolution electrical resistivity at the BC cribs and trenches site, Hanford. *Vadose Zone Journal*, **6**, 946–958.
- Rucker, D.F., Levitt, M.T. & Greenwood, W.J. (2009) Three-dimensional electrical resistivity model of a nuclear waste disposal site. *Journal of Applied Geophysics*, **69**, 150–164.
- Rucker, D.F., Loke, M.H., Noonan, G.E. & Levitt, M.T. (2010) Electrical resistivity characterization of an industrial site using long electrodes. *Geophysics*, in press.
- Sheriff, R.E. (2002) *Encyclopedic dictionary of applied geophysics*, 4th edn. Society of Exploration Geophysicists, Tulsa, OK. 429p.
- Siegrist, R.L. & Hargett, D.L. (1989) Application of surface geophysics for location of buried hazardous wastes. *Waste Management & Research*, **7**, 325–335.
- Telford, W.M., Geldart, L.P. & Sheriff, R.E. (1995) *Applied Geophysics*, 2nd edn. Cambridge University Press, UK. 770p.
- U.S. Department of Energy-Richland Operations (DOE-RL). (1998) *Groundwater/Vadose Zone Integration Project Background Information and State of Knowledge*. DOE/RL-98-48 vol. II Rev. 0, Richland, WA.
- Ward, A.L., Gee, G.W., Zhang, Z.F. & Keller, J.M. (2004) *Vadose Zone Contaminant Fate-and-Transport Analysis for the 216-B-26 Trench*. Pacific Northwest National Laboratory, PNNL-14907. Richland, WA.
- Ward, S.H. (1990) *Geotechnical and Environmental Geophysics, Volume 2: Environmental and Groundwater*. Investigations in Geophysics, 5. Society of Exploration Geophysicists, Tulsa, OK. 343p.
- Ward, S.H. & Hohmann, G.W. (1988) Electromagnetic theory for geophysical applications. In: Nabighian, M.N. (ed) *Electromagnetic methods in applied geophysics. Investigations in Geophysics*, 3. Society of Exploration Geophysicists, Tulsa, OK. 513p.

Acknowledgements

The author gratefully acknowledges the support of Mark Benecke of CH2M Hill and Mark Sweeney of Pacific Northwest National Laboratory. This work was completed under contract DE-AC27-96RL13200 for the U.S. Department of Energy, Richland, WA. The work was completed while the author was employed by hydroGEOPHYSICS, Inc. in Tucson, AZ.